Available online at www.sciencedirect.com
ScienceDirect
Free Radical Biology & Medicine 42 (2007) 64–78
www.elsevier.com/locate/freeradbiomed

Original Contribution

Increased oxygen radical formation and mitochondrial dysfunction mediate beta cell apoptosis under conditions of AMP-activated protein kinase stimulation

Ying Cai, Geert A. Martens, Simon A. Hinke, Harry Heimberg, Daniel Pipeleers, Mark Van de Casteele *

Received 21 March 2006; revised 16 August 2006; accepted 19 September 2006
Available online 27 September 2006

Abstract

AMP-activated protein kinase influences cellular metabolism, glucose-regulated gene expression, and insulin secretion of pancreatic beta cells. Its sustained activation by culture at low glucose concentrations or in the presence of 5-aminoimidazole-4-carboxamide riboside (AICAR) was shown to trigger apoptosis in beta cells. This study shows that both low glucose- and AICAR-induced apoptosis are associated with increased formation of mitochondrial superoxide-derived radicals and decreased mitochondrial activity. Mitochondrial dysfunction was reflected by an increased oxidized state of the mitochondrial flavins (FMN/FAD) but not of NAD(P)H. It was accompanied by suppression of glucose oxidation and glucose-induced insulin secretion, while palmitate oxidation appeared unaffected. When the cellular accumulation of superoxide-derived radicals was quenched by the ROS scavengers vitamin E, *N*-acetylcysteine, or the SOD-mimetic compound MnTBAP, apoptosis was significantly inhibited. Both low glucose and AICAR also elevated the expression of BH3-domain-only Bcl-2 antagonists, and induced caspase-3 activation, causing caspase-dependent truncation of Bcl-2. Overexpression of recombinant human Bcl-2 prevented caspase-3 activation, endogenous Bcl-2 processing, and apoptosis, but did not attenuate oxygen radical formation, AMPK activation, or JNK phosphorylation. We conclude that apoptosis by prolonged AMPK activation in beta cells results from enhanced production of mitochondria-derived oxygen radicals and onset of the intrinsic mitochondrial apoptosis pathway, followed by caspase activation and Bcl-2 cleavage which may amplify the death signal.

Keywords: Oxygen radicals; Mitochondria; AMPK; Bcl-2; Apoptosis; Diabetes; Beta cell

Introduction

Metabolic activity is crucial to the survival of pancreatic beta cells in vitro [1]. Conditions under which AMP-activated protein kinase (AMPK) is stimulated in beta cells are associated with a reduced biosynthetic and functional state of the cells. This has been demonstrated for culture in low glucose concentrations or in the presence of the AMPK activators 5-aminoimidazole-4-carboxamide riboside (AICAR) and metformin, as well as for adenovirus-mediated expression of constitutively active (CA)-AMPK [2–7]. We and others showed that when this state is prolonged in vitro, insulin producing MIN6 cells and primary beta cells die via an apoptosis program that is dependent on the activation of AMPK [3–5,7] and involves c-Jun N-terminal kinase [4]. AMPK-mediated apoptosis has been reported in other cell types [8–12]. Conversely, it is recognized that activation of the kinase leads to metabolic alterations that can prevent ATP depletion in certain cell types [13–15] resulting in improved survival under stress conditions and protection from apoptosis [16–20]. Beneficial effects of the AMPK activator metformin have been reported in human pancreatic islets exposed to high free fatty acid levels in vitro [21]. In view of its wide range of cellular effects, AMPK holds

Abbreviations: BSA, bovine serum albumin; AICAR, 5-aminoimidazole-4-carboxamide riboside; AMPK, AMP-activated protein kinase; DMEM, Dulbecco's modified Eagle's medium; FCS, fetal calf serum; GSIS, glucose-stimulated insulin secretion; H_2-DCFDA, dihydrodichlorofluorescein diacetate; DHE, dihydroethidine; MFI, mean absolute fluorescence intensities; MTT, 3-(4,5-dimethylthiazolyl-2)-2,5-diphenyltetrazolium bromide; NAC, *N*-acetylcysteine; ROS, reactive oxygen species; RT-PCR, reverse transcriptase-polymerase chain reaction; MTT, (3-(4,5-dimethylthiazolyl-2)-2,5-diphenyltetrazolium bromide; SOD, superoxide dismutase.

* Corresponding author. Fax: +32 2 477 4545.
E-mail address: mvdcaste@vub.ac.be (M. Van de Casteele).

0891-5849/$ - see front matter © 2006 Elsevier Inc. All rights reserved.
doi:10.1016/j.freeradbiomed.2006.09.018

promise as a therapeutic target in diabetes and cancer [22,23]. It is unclear how cell dysfunction and apoptosis can result from AMPK activation. This knowledge could be useful for minimizing the detrimental effects that are associated with a persistent kinase stimulation in beta cells [7]. On the other hand, it may be useful to promote these effects in cancer cells [22].

Sustained AMPK activation in beta cells and MIN6 cells can be provoked by culture in low glucose or in the presence of the AMPK stimulator AICAR [23]. These models have been used to identify mechanisms that contribute to AMPK-mediated beta cell death [3–5]. We recently found that production of reactive oxygen species in beta cells is increased when extracellular glucose is low or when mitochondrial metabolic activity is decreased [24]. In this study we investigate the putative involvement of ROS production and mitochondrial dysfunction in AMPK-mediated apoptosis of beta cells.

Materials and methods

Cell culture

Rat pancreatic beta cells were isolated by flow cytometry [25] and precultured overnight in suspension or as adherent cells in Ham's F10 medium (Invitrogen, Life Technologies, Inc., Paisley, Scotland) containing glucose (10 mM), 1% (wt/vol) charcoal-treated BSA (Sigma, St. Louis, MO), L-glutamine (2 mM), IBMX (50 μM), penicillin (0.075 mg/ml), and streptomycin (0.1 mg/ml), as previously described [26]. Subsequently, beta cells were cultured either in 10 or 3 mM glucose, or in 10 mM glucose containing AICAR (1-2 mM), for the indicated time periods. Mouse insulin-producing MIN6 cells (passages 20-32) were cultured in Dulbecco's modified Eagle's medium (DMEM) containing 15% (v/v) heat-inactivated fetal calf serum (FCS), as described [27]. At 60-70% confluency, MIN6 cells were exposed to 25 mM glucose (control conditions), 0.6 mM glucose (low glucose conditions), or 2 mM AICAR (in 25 mM glucose), always in DMEM containing 15% FCS [4]. The general caspase inhibitor z-VAD-fmk (Bachem, Bubendorf, Switzerland) was added to cell cultures at a concentration of 50 μM, 1 h before transferring the cells to apoptogenic culture conditions. The compounds vitamin E (5-25 μM; Merck, Darmstadt, Germany), NAC (*N*-acetylcysteine; 1 mM; Sigma), and the superoxide dismutase (SOD) mimetic compound MnTBAP (manganese(III)tetrakis(4-benzoic acid)porphyrin; 10-20 μM, Alexis Biochemicals, Lausen, Germany) were added to the cultures to decrease intracellular reactive oxygen species. Pyruvate (5-20 mM; Merck), which can be metabolized by MIN6 cells, was used for replacing glucose as metabolic fuel [28].

Insulin measurements

MIN6 cells were cultured for 24 h under the indicated conditions, washed, and cultured in KRHB medium without glucose for 1 h, followed by incubation for 2 h in KRHB medium (comprising 116.4 mM NaCl, 1.8 mM $CaCl_2$, 0.8 mM $MgSO_4$, 5.4 mM KCl, 1.02 mM NaH_2PO_4, 0.075 mM BSA, 26.2 mM $NaHCO_3$), at different glucose concentrations (0, 5, 10, or 25 mM). At the end of culture, medium was taken for measurement of insulin release, and cells were collected for analysis of their insulin content. Secreted insulin and total cellular insulin were measured by radioimmunoassay, as previously described [29].

Glucose and palmitate oxidation

MIN6 cells were precultured for 24 h under the indicated conditions. CO_2 formation from glucose and palmitate was measured in duplicate samples of 10^5 MIN6 cells and incubated for 2 h at 37°C in 100 μl of the appropriate medium. Glucose metabolism was measured in Ham's F10 medium containing 0.5% BSA, 2 mM L-glutamine, 10 mM Hepes, and 10 mM D-glucose (5 μCi D-[U-^{14}C]glucose). Palmitate metabolism was measured in KRBH medium, containing 0.2% BSA (fraction V), 2 mM calcium, 10 mM Hepes, 0.5 μCi [U-^{14}C]palmitic acid, and unlabeled palmitate up to a final concentration of 50 μM. Cells were incubated at 37°C in a glass siliconized tube trapped in an airtight glass vial. After 2 h, the metabolism was stopped by injecting 20 μl HCl 1 N, and 250 μl hydroxyhiamine (Packard Bioscience, Groningen, The Netherlands) was used to capture the produced $^{14}CO_2$ for 1 h at room temperature. D-[U-^{14}C]Glucose or [U-^{14}C]palmitic acid oxidation rates were determined by liquid scintillation counting of the generated $^{14}CO_2$.

Measurement of redox state

The metabolic redox state of MIN6 cell populations was analyzed after 30-min incubation in humidified air (20% O_2/5% CO_2) at 37°C. It was determined by flow cytometry measuring cellular fluorescence of NAD(P)H (argon laser 351–363/400–470 nm) and mitochondrial riboflavin (FAD and FMN, argon laser 488/530 nm) using a dual-laser FACStar Plus system (BD Biosciences) [30]. Mean absolute fluorescence intensities (MFI) were measured for 10,000 propidium iodide (PI, 5 μg/ml)-negative cells. Cellular NAD(P)H and flavin fluorescence was measured in cells cultured in 25 mM glucose or 0.6 mM glucose, either with or without AICAR. Brief exposure (5 min) to antimycin A (Sigma-Aldrich) was used as a positive control. Data were expressed relative to the MFI of control MIN6 cell populations cultured in 25 mM glucose.

Measurement of H_2O_2 and superoxide

The production of reactive oxygen species (ROS) in MIN6 cells was measured as recently described for beta cells [24]. Briefly, MIN6 cells cultured in 24-well plates (3-5 × 10^5 cells per well) were incubated for 1 h with the cell-permeable fluorescent ROS-probe dihydrodichlorofluorescein diacetate (H_2-DCFDA; 10 μM), or for 20 min with the superoxide probe dihydroethidine (DHE; 2.5 μM; Molecular Probes, Invitrogen), after which the cells were washed in DMEM and collected. Cellular fluorescence derived from oxidized probes was measured by FACS [24]. FACS data were presented as the mean fluorescence

intensity of the cell population, and normalized by the MFI value of cells cultured under control conditions (25 mM glucose).

Mitochondrial activity

Reduction of MTT (3-(4,5-dimethylthiazolyl-2)-2,5-diphenyltetrazolium bromide) to insoluble formazan by mitochondrial dehydrogenases can be used to measure mitochondrial nutrient metabolism in many cell types, and correlates well with glucose oxidation in pancreatic β-cells [31,32]. The MTT reduction assay was used to examine the mitochondrial activity and metabolic effects of glucose limitation and AICAR in MIN6 cells. Briefly, cells were seeded at 25,000 cells/well into 96-well plates and grown for 3 days. The amount of 10 μl of MTT (5 mg/ml in PBS) was added, and the incubation was allowed to proceed for an additional 2 h. Insoluble precipitated formazan produced was dissolved in 100 μl dimethyl sulfoxide following 10 min centrifugation of the microtiter plate at 3000 rpm/4°C and removal of the supernatant. Absorbance was measured on a Wallac Victor^2 microplate reader at 490 nm. Data are expressed as absorbance (A_{490}) values and normalized to the parallel control response of cells incubated for the identical time period in 25 mM glucose.

Plasmids

Empty vector pEF1 (pEF1/V5-HisA) and the recombinant plasmids pNLS-EGFP, pCAGGS-p35, pEF1-crmA (pEF1/V5-HisA-crmA), and pEF1-hBcl-2 (pEF1/V5-HisA-hBcl-2) expressing respectively the GFP, baculovirus p35, cowpox crmA, and human Bcl-2 gene were a gift from Dr. P. Vandenabeele (Ghent University, Belgium) or obtained from the Belgian coordinated collections of microorganisms (BCCM): laboratory of molecular biology-plasmid collection (LMBP). They were amplified in *Escherichia coli* (Strain: DHSK-F) and isolated using NucleoBond columns (Machery-Nagel, Gutenberg, Germany).

Transient transfections

MIN6 cells were cultured to 60–70% confluence in 6-well plates and were transfected with 1 μg of plasmid DNA using Lipofectamine Plus reagents according to the manufacturer's instructions (Invitrogen, Paisley, Scotland). To each well, 0.5 μg of a plasmid expressing nuclearly targeted green fluorescent protein (pNLS-EGFP) together with 0.5 μg of plasmid expressing crmA, p35, or human Bcl-2 cDNA were applied. After lipid-mediated DNA transfection for 3 h, cells were cultured for 24 h in normal medium, and then cultured under apoptogenic or control conditions.

Generation of stable MIN6 cell transfectants

MIN6 cells were transfected either with empty vector pEF1, or with plasmid pEF1-hBcl-2, as described above. The cells were reseeded 24 h later as single cells, and cultured for 5 weeks in the presence of 400 μg/ml geneticin G418 (Invitrogen). Neo^R (neomycin resistant) cell colonies were picked up from the culture substratum under an inverted microscope using a sterile siliconized Pasteur pipette and transferred to selective medium (200 μg/ml G418) for expansion. The Neo^R cells were examined for expression of human Bcl-2 protein by Western blotting, before they were used in further experiments. The hBcl-2 protein content in each Neo^R line remained stable for at least 2 months.

Assay of apoptosis and caspase-3 activity

Living, apoptotic and necrotic MIN6 cells were identified by fluorescence microscopy, using propidium iodide (10 μg/ml, Sigma) and Hoechst 33342 (10 μg/ml, Sigma), as previously described for beta cells [1]. In p-NLS-EGFP-transfected cells, nuclear morphology was directly examined under the fluorescence microscope (see Fig. S4). Apoptotic cells (<2*n* DNA; sub-G1 cells) were also identified and counted by FACS, as described [33]. Activity of caspase-3 enzyme in MIN6 cells was determined using the fluorigenic substrate AC-DEVD-AMC [4]. Caspase-3 activity was expressed as the number of arbitrary fluorescence units (AMC fluorescence; 505 nm) measured per milligram protein and per hour.

mRNA extraction and RT-PCR

Polyadenylated RNA was extracted from MIN6 cells or from rat primary beta cells using poly(dT)-coated magnetic microbeads (Dynabeads, Dynal A.S, Oslo, Norway). Reverse transcription and PCR amplification were carried out using the GeneAmp RNA PCR kit (Perkin-Elmer Applied Biosystems). Negative RT-PCR controls consisted of reactions without reverse transcriptase. The oligonucleotide primers (Invitrogen) used in this study, are listed in Table 1. Each PCR involved a 2-min initial denaturation step at 94°C, followed by 26–32 cycles with stages at 94°C for 30 s, at 55–65 °C for 30 s, and at 72°C for 1 min. PCR products were visualized on 1.2% agarose gels stained with ethidium bromide, and the signals recorded and quantified as previously described [27].

Western blot analysis

Cellular protein was extracted by a 1-min sonication in RIPA buffer [34]. Protein concentration was determined by the micro-BCA assay (Pierce, Rockford, IL) using bovine serum albumin as the standard. Samples (25 μg protein) were mixed with SDS loading buffer and boiled, separated on 12 or 15% SDS-polyacrylamide gels and proteins were transferred to a nitrocellulose membrane (Schleicher and Schuell Bioscience, Dassel, Germany).

Specific antibodies recognizing the following proteins or epitopes were used: casp-3 (gift from Dr. P. Vandenabeele), human-Bcl-2 (ΔC 21), mouse-Bcl-2 (N-19) (Santa Cruz Biotechnology, Santa Cruz, CA), phospho-(Thr 183/Tyr 185)-c-jun-N-terminal kinase (JNK), total JNK (New England Biolabs, Beverly, MA), phospho-(Thr 172)-AMPK (Cell Signaling

Table 1
Properties of primers used for RT-PCR on mRNA of MIN6 cells (M) or rat beta cells (R)

Gene	Sense, antisense	Primer sequence	Annealing temperature (°C)	Product size (bp)
A1/Bfl-1 (M)	S	5′-AAAGAGTTGCTTTCTCCG-3′	55	314
	A	5′-ATCTTCCCAACCTCCATT-3′		
A1/Bfl-1 (R)	S	5′-AATCGGCTCCAAGCAAAA-3′	60	290
	A	5′-CGCCACAAAACTGGAAA-3′		
Bad (M/R)	S	5′-ATGTTCCAGATCCCAGAGTT-3′	55	452 (M)
	A	5′-CGATCCCACCAGGACTGGA-3′		455 (R)
Bak (M/R)	S	5′- ATGGCATCTGGACAAGGA-3′	55	340 (M)
	A	5′-TGGAGGCGATCTTGGTGAA-3′		343 (R)
Bax (M/R)	S	5′-GAACCATCATGGGCTGGACA-3′	55	179
	A	5′-TCAGCCCATCTTCTTCCAGA-3′		
Bcl-2 (M/R)	S	5′-AAAAAGAGGGGGGGCAAA-3′	60	441 (M)
	A	5′-AATCCGTAGGAATCCCAA-3′		462 (R)
Bcl-xl (M/R)	S	5′-GCCCATCTCTATTATAAAAAT-3′	55	472 (M)
	A	5′-CACAGTGCCCCGCCAAAGGAG-3′		471 (R)
Bid (M/R)	S	5′-AAGACGAGCTGCAGACA-3′	55	314
	A	5′- TTTGGCCAACAGCATTGT-3′		
Bim (M/R)	S	5′-GGTAATCCCGACGGCGAAGGGAC-3′	55	160
	A	5′-AAGAGAAATACCCACTGGAGGACC-3′		
DP-5/Hrk (M/R)	S	5′-GGACCGAGCAACAGGTT-3′	55	267 (M)
	A	5′-TGTGGAAAGGAAAGGGA-3′		271 (R)
DP-5/Hrk (R)	S	5′-AGCAACAGGTTGGCGAAA-3′	55	175
	A	5′-TAAATAGCACTGAGGTGG-3′		
Mcl-1 (M/R)	S	5′- GGCATGCTCCGGAAACT-3′	55	263
	A	5′-TCCACAAACCCATCCCA-3′		
Noxa (M)	S	5′-TGAGATGCCCGGGAGAAA-3′	55	182
	A	5′-TCATCCTGCTCTTTTGCGA-3′		
Catalase (M/R)	S	5-TCTGCAGATACCTGTGAACTG-3′	60	357
	A	5′-TAGTCAGGGTGGACGTCAGTG-3′		
Glutathione peroxidase (M)	S	5′-CTCGGTTTCCCGTGCAATCAG-3′	65	431
	A	5′-GTGCAGCCAGTAATCACCAAG-3′		
Heat shock protein 70 (M)	S	5-ACGCAGACCTTCACCACC-3′	60	278
	A	5′-CGCTCGATCTCCTCCTTG-3′		
Beta actin (M/R)	S	5′-CGTGGGCCGCCCTAGGCACCA-3′	55	242
	A	5′-TGGCCTTAGGGTTCAGAGGGG-3′		

Technology, Beverly, MA), heme oxygenase (HO-1, Stressgen, Victoria, BC, Can), heat shock protein 70 (HSP70, Stressgen), and β-actin (Santa Cruz Biotechnology). The appropriate secondary antibodies conjugated with horseradish peroxidase were applied, and immunoreactivities revealed by enhanced chemiluminescence (Amersham Bioscience, Bucks, UK).

Statistical analysis of data

Quantitative data are presented as the mean ± SE of at least three independent experiments. Statistical analysis of data was done by Student's *t* test, or by one-way ANOVA using Dunnett's test in multiple comparisons of means. Differences were considered statistically significant if the p value was <0.05.

Results

Low glucose or AICAR cause mitochondrial dysfunction and increased formation of oxygen radicals

We analyzed production of oxygen radicals in living (propidium iodide negative) MIN6 cells cultured in either a low glucose concentration or in the presence of the AMPK activator AICAR.

As a first approach, we measured ROS by following the cellular oxidation of dihydrodichlorofluorescein diacetate, a probe which is oxidized to green fluorescent DCF by various peroxide-like ROS and nitric-oxide-derived reactive intermediates [35]. In H_2-DCFDA-loaded MIN6 cells, the mean DCF fluorescence was increased 1.7-fold by culture for 24 h in 0.6 mM glucose, as compared to MIN6 cells cultured under the 25 mM glucose control condition ($P < 0.02$ vs control; Fig. 1A). A 1.7-fold increase of the mean DCF fluorescence was also seen in cells cultured for 24 h in the presence of AICAR ($p < 0.05$ vs control; Fig. 1A). We next used the superoxide-selective [36,37] probe dihydroethidine to examine the superoxide anion production in individual MIN6 cells by FACS. This showed that the increased H_2-DCFDA oxidation was associated with a markedly increased mitochondrial superoxide formation as measured by DHE (Supplementary Fig. S1). These results indicated a sustained increase of superoxide(-derived) ROS production under both low glucose and AICAR conditions. Accordingly, the mRNA expression of antioxidant enzymes glutathione peroxidase and catalase was significantly increased at 24 h of culture in low glucose or AICAR, while the mRNA expression of heat shock protein Hsp-70 was unaltered (Fig. 1B). Cellular expression of heme oxygenase-1 (HO-1) protein, an inducible enzyme capable of cytoprotection via radical

scavenging in beta cells [38], was also increased under both conditions (Fig. 1C).

The MTT (tetrazolium) colorimetric assay was used to measure mitochondrial activity (MTT-reducing potential) in MIN6 cells [31,32]. This showed that mitochondrial function was significantly inhibited at ≥12 h of culture in low glucose or in the presence of AICAR, as compared to culture in 25 mM glucose (Fig. 1D).

Chronic exposure (24 h) to AICAR in either 25 mM or low glucose did not affect NAD(P)H in MIN6 cells (Fig. 1E). In

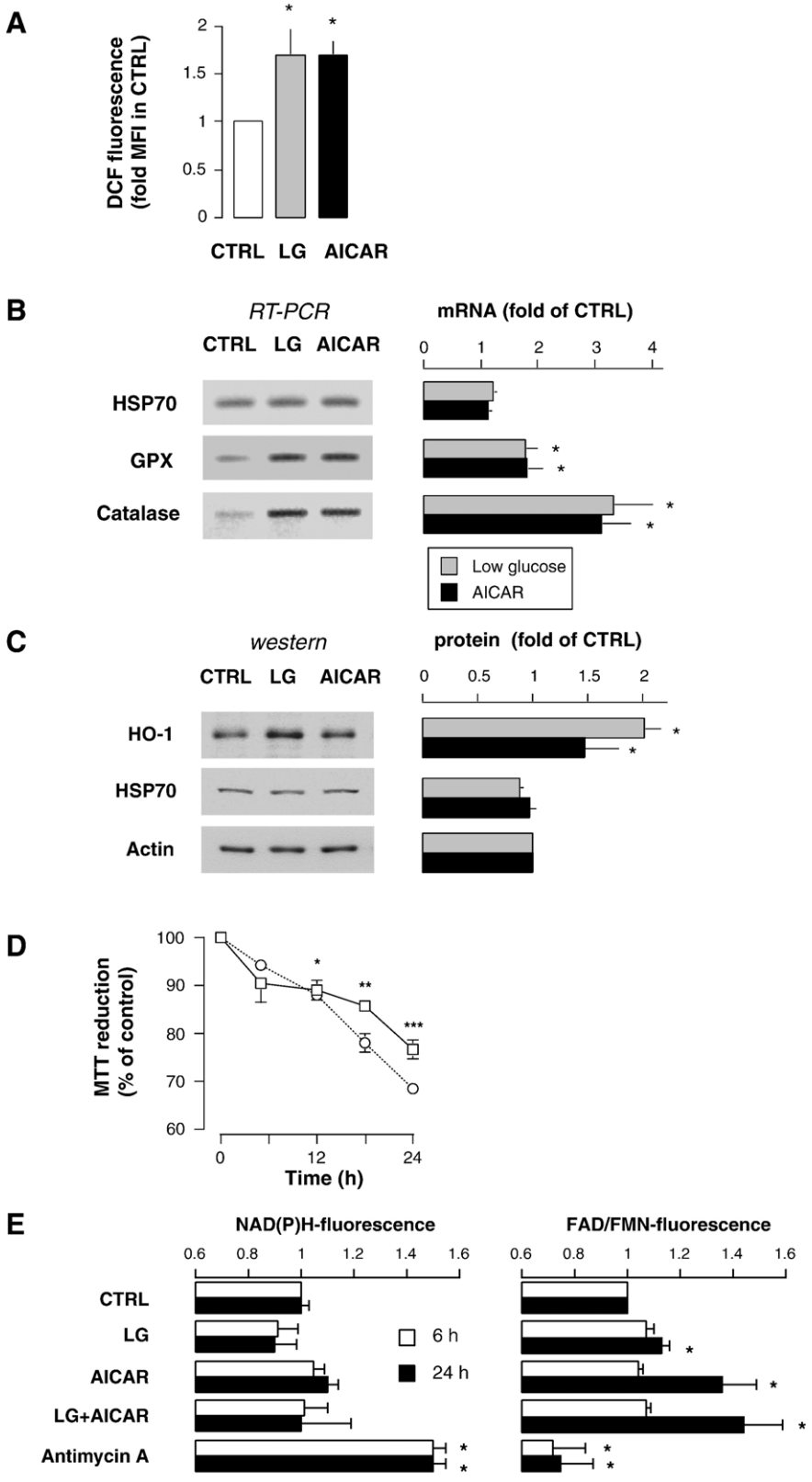

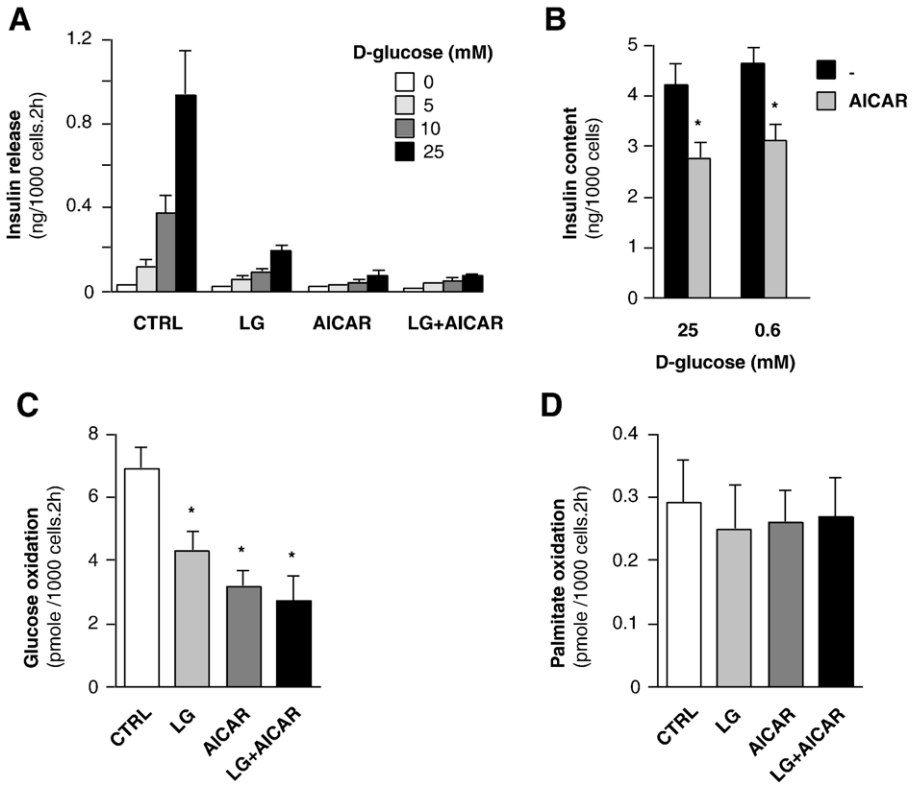

Fig. 2. Effect of low glucose or AICAR treatment on glucose-stimulated insulin secretion (GSIS), insulin content, glucose oxidation, and free fatty acid oxidation. (A) MIN6 cells were cultured for 24 h, in 25 mM glucose (CTRL) or 0.6 mM glucose (LG), with or without AICAR (2 mM). Insulin secretion was then measured during incubation of cells for 2 h in KRHB medium supplemented with the indicated glucose concentrations. Released insulin was quantified ($n = 4$) by radioimmunoassay, as described under Materials and methods. (B) Cells were then collected and their insulin content was analyzed. AICAR lowered the insulin content in both 25 and 0.6 mM glucose; *$p < 0.05$ vs no AICAR (−), $n = 4$. (C, D) MIN6 cells were cultured for 24 h as in A and their rates of glucose oxidation (C) and palmitate oxidation (D) were measured as described under Materials and methods. *$p < 0.05$ vs CTRL, $n = 3$−5.

contrast with the absence of effect on NADH, AICAR altered the riboflavin oxidation status: 24-h exposure resulted in a marked increase in oxidized FAD/FMN in abundant (25 mM) glucose (Fig. 1E), probably reflecting decreased levels of reduced $FADH_2$/$FMNH_2$. This also occurred in glucose-deprived cells (Fig. 1E). Cellular NAD(P)H and FAD/FMN were unaffected by 6-h exposure to AICAR, low glucose, or a combination of both (Fig. 1E). Increased superoxide production and inhibition of mitochondrial activity also required >6 h (Fig. 1D, and not shown). Thus, conditions that activate AMPK increase the oxidized state of mitochondrial flavins, but do not affect NAD(P)H formation. This redox imbalance correlates with increased superoxide formation and mitochondrial dysfunction in beta cells.

Low glucose or AICAR inhibit glucose-stimulated insulin secretion (GSIS) and cellular oxidation of glucose but not of palmitate

We next examined whether these mitochondrial effects functionally disabled the MIN6 cells. Exposure of MIN6 cells to low glucose (0.6 mM) for 24 h markedly reduced their GSIS (Fig. 2A). Exposure to AICAR (2 mM) in either normal glucose (25 mM) or low glucose (0.6 mM) resulted in nearly complete

Fig. 1. Stimulation of peroxide-like ROS production in MIN6 cells. (A) MIN6 cells were cultured for 24 h in 0.6 mM glucose (LG), or in 25 mM glucose either without (CTRL) or with 2 mM AICAR, and peroxide-like ROS was detected with H_2DCFDA by flow cytometry (see Materials and methods). Data (mean ± SE, $n = 6$) for DCF oxidation in cells are normalized by expressing the mean fluorescence index (MFI) for the respective cell population relative to the MFI of the control population (CTRL). (B) mRNA expression of glutathione peroxidase (GPX), catalase, and heat shock protein 70 (HSP70) was analyzed by RT-PCR (for PCR primers see Table 1). Actin was used as internal control (not shown). Data in the right panel (mean ± SE, $n = 4$) are expressed as fold mRNA under control conditions (*$p < 0.05$ vs CTRL). (C) Western blotting for heme oxygenase-1 (HO-1), HSP-70, and actin was performed using specific antibodies (see Methods). Data in the right panel (mean ± SE, $n=3$) are expressed as fold protein under control conditions (*$p < 0.05$ vs CTRL). (D) Time-dependent inhibition of MIN6 cell mitochondrial activity by glucose limitation (square symbols) or addition of 2 mM AICAR (circles). Mitochondrial activity was measured using the MTT-reduction assay. MTT was added to cell culture wells 2 h prior to the endpoint, and the formazan produced was measured spectrophotometrically at 490 nm. Data represent the mean ± SE of 4–7 experiments (*$p < 0.05$, **$p < 0.01$, ***$p < 0.001$). (E) MIN6 cells were cultured for 24 h as described in A, or in the presence of antimycin A (200 nM, 5 min). Using FACS, NAD(P)H fluorescence (left) and riboflavin (FAD-FMN) fluorescence (right) were subsequently measured in populations of dispersed MIN6 cells, as described under Materials and methods. As positive control for the NAD(P)H measurement a 5-min exposure to complex III inhibitor antimycin was included. Data represent average mean fluorescence index (MFI) ± SE normalized to MFI in control (25 mM glucose). *$p < 0.05$ vs CTRL, $n = 4$.

suppression of GSIS (Fig. 2A). The inhibition of GSIS by 24 h culture in low glucose did not result in an increased cellular insulin content, as compared to culture in 25 mM glucose (Fig. 2B). The insulin content of MIN6 cells cultured in the presence of AICAR was decreased by ±30% (Fig. 2B). These data confirm earlier published results showing that AMPK activation inhibits insulin biosynthesis [5] and release [6]. They also suggest that AMPK inhibition of GSIS is not primarily mediated by changes in the cellular insulin stores. Since GSIS is dependent on mitochondrial oxidative activity, we next examined whether AMPK activation affected the glucose-oxidation rate of MIN6 cells. The data in Fig. 2C show that preexposure of the cells to low glucose, AICAR, or a combination of both decreased their glucose-oxidation rate by 50–70%. Under the same conditions, the rate of palmitate oxidation was unaltered (Fig. 2D). The results indicate that AMPK activation decreases the oxidation of glucose-carbon in the mitochondria, apparently without compensatory increase in the oxidation of free fatty acids. This is consistent with the observed reduction in mitochondrial activity (MTT assay) and with the suppression of GSIS.

Low glucose- or AICAR-induced ROS formation results in apoptosis

As we previously reported [4], MIN6 cells exposed to either a low glucose concentration (0.6 mM) or to AICAR (2 mM) underwent apoptosis (Fig. 3A). This effect was seen at 24 h and was more pronounced at 48 h (Fig. 3A), while necrosis affected less than 1% of the cells under these conditions (Fig. 3B). To examine whether the increased ROS formation participated in apoptosis onset, MIN6 cells were exposed to low glucose for 24 h in the absence or presence of ROS scavengers, and apoptosis rates were determined by FACS. The compounds vitamin E (5 μM), *N*-acetylcysteine (1 mM), and the superoxide dismutase mimetic MnTBAP (10 μM) all scavenged ROS (Fig. 4A) and prevented apoptosis (Fig. 4B) induced by low glucose. In addition, the metabolic fuel pyruvate (5-10 mM) could substitute for glucose in that it also suppressed both ROS production and apoptosis in MIN6 cells (Figs. 4A and B). With

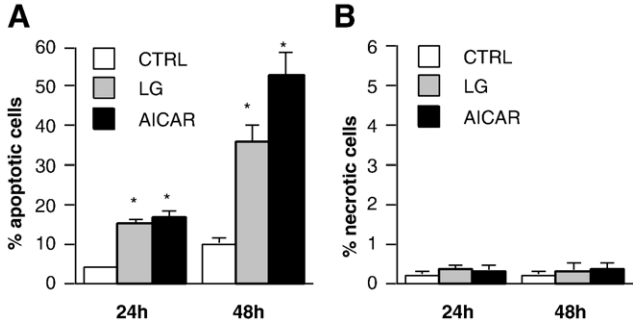

Fig. 3. Low glucose concentrations or AICAR induce apoptosis in MIN6 cells. Cells seeded in 96-well plates were exposed to medium containing either 25 mM glucose (CTRL), 0.6 mM glucose (LG), or 2 mM AICAR, for 24 or 48 h. The percentages of (A) apoptotic and (B) necrotic cells were determined by direct counting under the fluorescence microscope after propidium iodide and Hoechst staining. Data represent the mean ± SE of 5 independent experiments. *$p < 0.01$ vs CTRL.

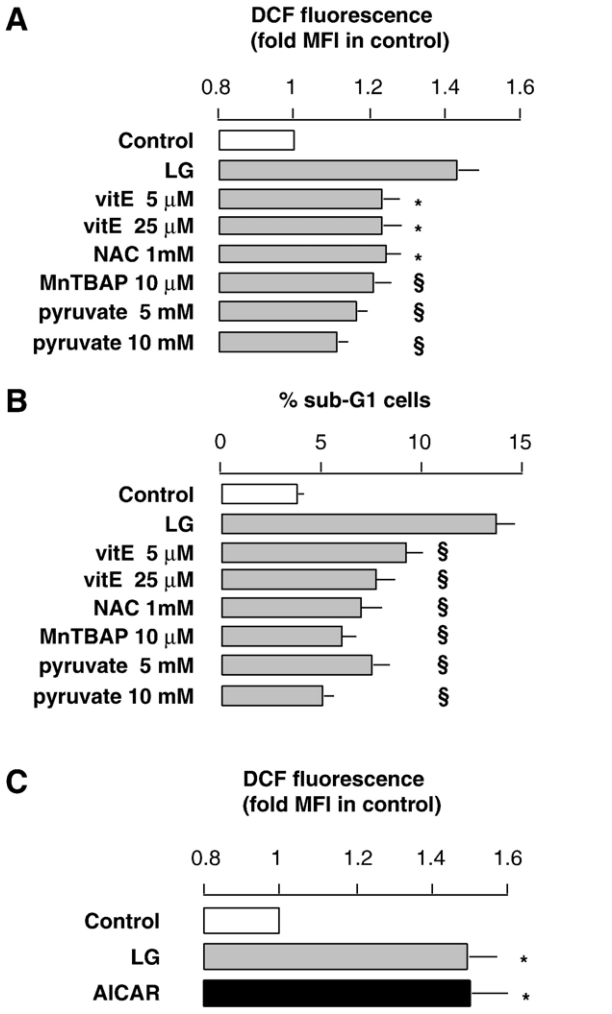

Fig. 4. ROS species are early mediators of the apoptosis. MIN6 cells were cultured for 24 h under control conditions (CTRL) or in low glucose (LG) as well as in LG supplemented with chemical ROS scavengers vitamin E (vitE), *N*-acetylcysteine (NAC), pyruvate, and the SOD-mimetic compound MnTBAP, as indicated. (A) ROS was measured by FACS analysis and the data ($n = 8–10$, mean ± SE, *$p < 0.02$, § $p < 0.01$ vs LG) were expressed as in Fig. 1. (B) DNA degradation was measured by FACS using the fluorescent probe propidium iodide. Data ($n = 6–12$; § $p < 0.01$ vs LG) are expressed as the percentage of cells with <2*n* DNA (% sub-G1 cells). (C) ROS production was not inhibited in Neo^R B1 cells expressing hBcl-2 ($n = 5$; *$p < 0.01$ vs CTRL).

the exception of vitamin E, the scavengers used here to suppress apoptosis also inhibited the accumulation of superoxide (Supplementary Fig. S1).

Increased expression of BH3-only proteins may activate and ectopic expression of hBcl2 inhibits an intrinsic apoptosis pathway under conditions of AMPK activation

Low glucose or AICAR induce apoptosis only when applied for ≥ 24 h in MIN6 cells and beta cells (Fig. 3A, and [3,4]). It is unknown whether alteration in gene expression by AMPK activation can contribute to mitochondrial dysfunction and cell death. BH3-domain-only proteins are transcriptionally regulated inhibitors of the antiapoptotic function of Bcl-2 in several systems [39]. We used semiquantitative RT-PCR to measure the

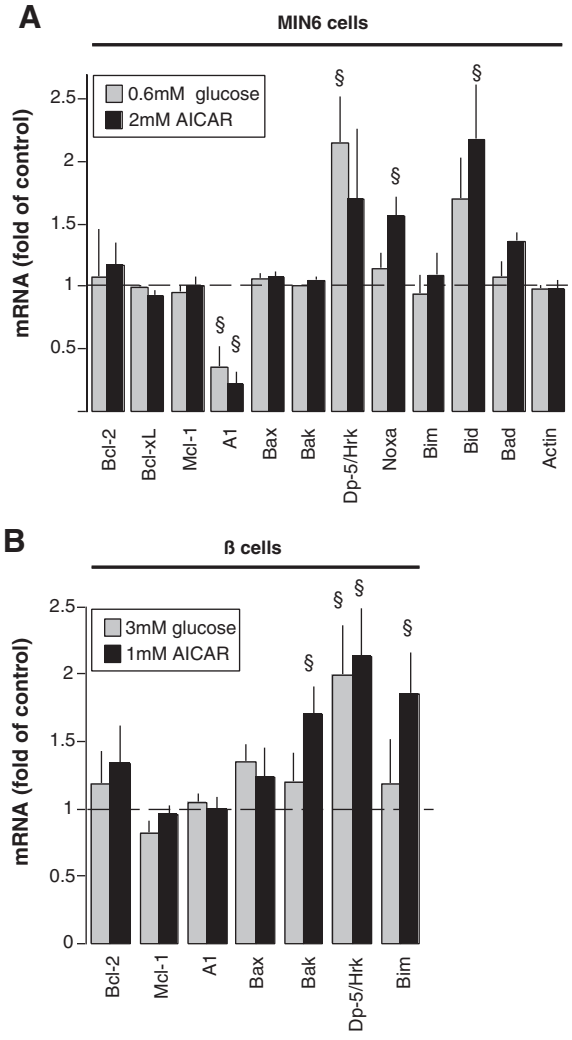

Fig. 5. RT-PCR analysis of Bcl-2-family genes. (A) MIN6 cells and (B) primary beta cells were cultured in medium containing low glucose or AICAR for 24 h. mRNA was isolated and subjected to semiquantitative RT-PCR using specific primers (see Table 1). Data are expressed as fold mRNA in control cells, and represent the mean ± SE of 4–5 experiments in A and 5–8 experiments in B. *$p < 0.05$ vs control.

Bcl-2 family gene expression at 24 h of culture in low glucose or AICAR. In MIN6 cells, the proapoptotic BH-3-only members DP-5/Hrk and Bid were up-regulated, and antiapoptotic A1-mRNA was decreased under both conditions. Proapoptotic BH-3-only Noxa mRNA was also increased in AICAR (Fig. 5A). In primary beta cells, DP-5/Hrk was again up-regulated by both low glucose and AICAR, while the BH3-only family member Bim, and death agonist Bak, were also increased in AICAR (Fig. 5B). Antiapoptotic homologues Bcl-2, Bcl-xL, and Mcl-1 were not significantly altered in MIN6 cells (Fig. 5A) or in beta cells (Fig. 5B). Thus, under conditions of AMPK activation and concomitant with cell death induction, the expression of proapoptotic BH3-only mRNA is up-regulated consistently for DP5/Hrk. Depending on the cell type, AICAR additionally induces Bid, Bim, or Noxa. Together, the results suggest a role for BH3-only members of the Bcl-2 family in AICAR and low glucose-induced apoptosis.

To investigate the involvement of mitochondrial mediators in the onset of apoptosis in these models, MIN6 cells that stably expressed the human Bcl-2 protein (hBcl-2) were generated. MIN6 cells were transfected with empty vector (pEF1) or with plasmid pEF1-hBcl-2 and maintained in G418 (400 µg/ml). Neomycin/geneticin-resistant (Neo^R), clonally expanded cells were thus obtained that either stably expressed h-Bcl2 (B1, 3, 6, 7, and 9; Fig. 6A) or were negative for the protein (P1-4; Fig. 6A). These cells were then exposed for 48 h to a low glucose concentration (0.6 mM) or to AICAR (2 mM) and apoptotic cells were counted using fluorescence microscopy (Fig. 6B) and by FACS measurement of cellular DNA degradation (Supplementary Fig. S2). This showed that both low glucose and AICAR induced apoptosis in Neo^R cells that did not express hBcl-2 (P1, 4; Fig. 6B), whereas apoptosis was inhibited in MIN6 cells expressing hBcl-2 (B1, 3, 6, 7; Fig. 6B). Cell death inhibition in hBcl-2-expressing cells was also evident in light microscopy (Supplementary Fig. S3). Thus, Bcl-2 potently counteracts apoptosis induction by low glucose or AICAR, suggesting that crucial cell death mediators derive from, or target, the beta cell mitochondria.

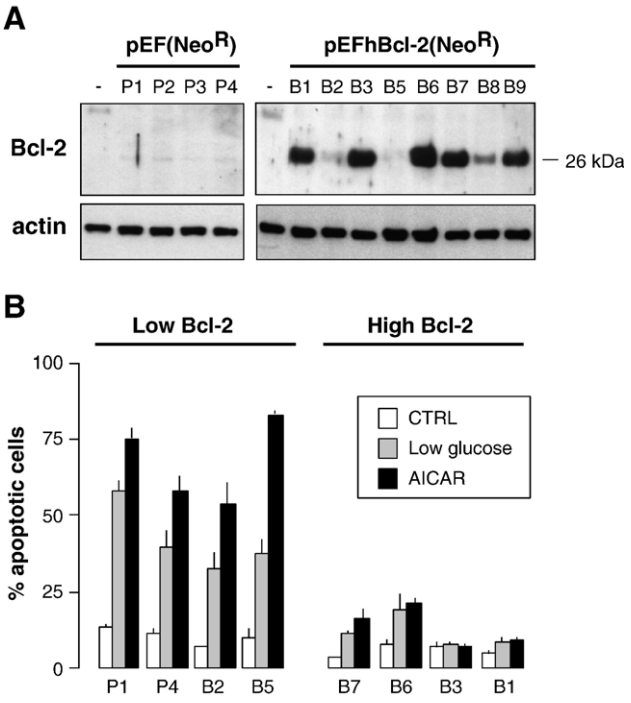

Fig. 6. High level expression of human Bcl-2 prevents low glucose and AICAR-induced apoptosis. Stable transfectants (Neo^R) expressing human Bcl-2 (hBcl-2) were obtained as described in the text. (A) Human Bcl-2 protein expression was detected with antibody specific for human Bcl-2 in Neo^R-resistant MIN6 cells that had been transfected with empty vector pEF1 (left panel, clones P1-P4) or with pEF1-hBcl2 (right panel, clones B1–3 and B5–9), or in nontransfected MIN6 cells (−). Clones B2 and B5 expressed detectable but low levels of hBcl-2 protein. (B) Apoptosis induction was assessed by cell counting under the fluorescence microscope (as in Fig. 3) in stable Neo^R clones that showed low or no hBcl-2 expression (left), and in clones that expressed high levels of hBcl-2 (right), after culture under control conditions, 0.6 mM glucose, or 2 mM AICAR, for 48 h. Data represent the mean ± SE of 4–6 independent experiments. Low glucose and AICAR both induced significant effects in clones P1, P4, B2, and B5 ($p < 0.01$ vs CTRL).

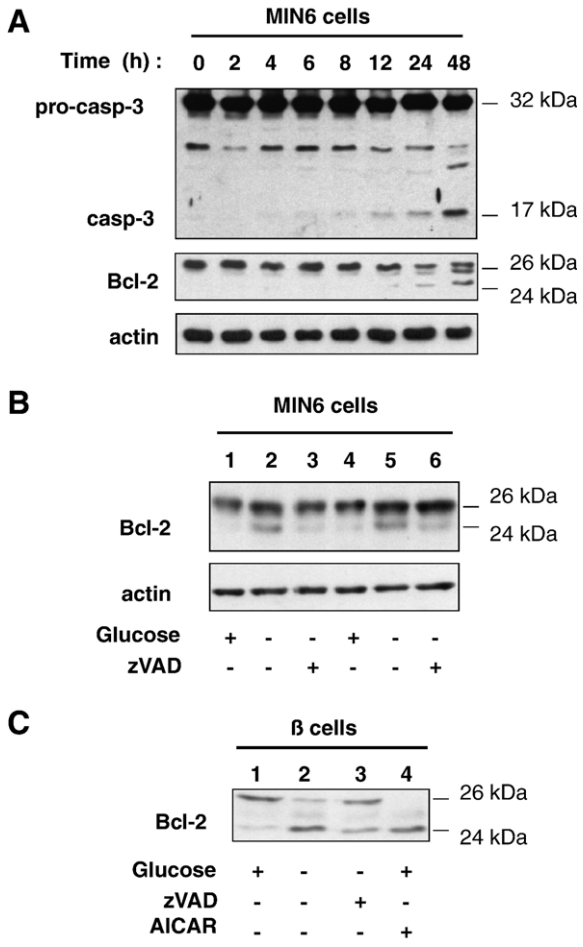

Fig. 7. Low glucose concentrations or AICAR induce casp-3 activation and Bcl-2-cleavage in beta cells. (A) Western blot showing the time course of proteolytic casp-3 activation and Bcl-2 cleavage in MIN6 cells exposed to 0.6 mM glucose. Pro (32 kDa) and activated (17 kDa) forms of casp-3 were detected using casp-3-specific antibody. The 26-kDa Bcl-2 protein as well as a 24-kDa Bcl-2 protein were detected at time points ≥24 h, using a Bcl-2-specific antibody. (B) MIN6 cells were cultured in 25 mM glucose (+) or in 0.6 mM glucose (−) for 24 h in the absence or presence of 50 μM of the general caspase inhibitor z-VAD-fmk, and the appearance of truncated Bcl-2 (24 kDa) was evaluated by Western blotting. Two experiments are shown (lanes 1–3 and 4–6). (C) Increased cleavage of Bcl-2 protein was detected in lysates of 2×10^5 rat beta cells that were cultured for 72 h in 3 mM glucose (lane 2) or 2 mM AICAR (lane 4), as compared to culture in 10 mM glucose (lane 1). z-VAD-fmk partially inhibited the Bcl-2 cleavage caused by the low glucose concentration (lane 3). Results shown are representative of 3–4 experiments.

Activation of caspase-3 and truncation of Bcl-2 contribute to apoptosis

In MIN6 cells, low glucose concentrations or AICAR induced a time-dependent proteolytic activation of caspase-3, paralleled by conversion of the 26-kDa Bcl-2 protein to a Bcl-2 protein of 24 kDa (Fig. 7A, and not shown). Low glucose-induced cleavage of the Bcl-2 protein was suppressed by addition of 50 μM of the broad-spectrum caspase-inhibitor z-VAD-fmk (Fig. 7B, lanes 2–3 and 5–6). In primary beta cells, Bcl-2 protein cleavage was induced by culture in 3 mM glucose (Fig. 7C, lanes 1–2) or in medium containing 10 mM glucose and 1 mM AICAR (Fig. 7C, lane 4), and was inhibited by zVAD-fmk (Fig. 7C, lanes 2–3). These data indicated that both AICAR and low glucose induced a caspase-dependent truncation of Bcl-2 in beta cells.

To evaluate whether specific caspase subtypes contribute to beta cell death, MIN6 cells were transiently transfected with plasmids encoding either baculovirus p35 protein (pCAGGS-p35) or cowpox CrmA protein (pEF1-crmA), known inhibitors of casp-3- and casp-1-like enzymes, respectively. Cotransfection with plasmid pNLS-GFP, which drives a nuclearly targeted GFP expression, allowed for direct microscopic counting of the percentage of transfected cells undergoing nuclear apoptosis (supplementary Fig. S4). In low glucose, apoptosis was decreased in MIN6 cells transfected with pCAGGS-p35, as compared to cells transfected with empty pEF1-vector or plasmid pEF1-crmA (Fig. 8). Similar results were obtained in the presence of AICAR (supplementary Fig. S4). Under these conditions, apoptosis was also inhibited by transfection with plasmid pEF1-hBcl-2 expressing recombinant human Bcl-2 (Fig. 8). The results suggest that activation of casp-3 but not of casp-1, and possibly the ensuing caspase-dependent truncation of Bcl-2, contributes to low glucose and AICAR-induced apoptosis.

Bcl-2 does not reduce ROS formation, or AMPK and JNK activation, but protects against caspase-3 activation and apoptosis

In response to long-term culture in low glucose or AICAR, the ROS production in MIN6 cells that stably expressed h-Bcl-2 protein was similar to that in control MIN6 cells (Fig. 4C). Thus, elevated ROS production contributes to apoptosis but is not influenced by increased Bcl-2 expression, indicating that ROS species are early mediators of apoptosis.

Although casp-3 is widely considered an executioner caspase, casp-3 activation coupled to Bcl-2 cleavage has been reported to initiate apoptosis in some systems [40]. We tested

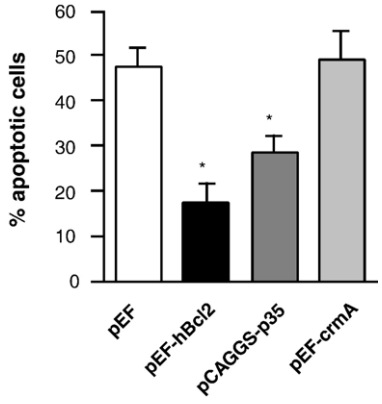

Fig. 8. Transient expression of Bcl-2 or p35 reduces apoptosis. MIN6 cells were transfected with 0.5 μg of plasmid pNLS-EGFP encoding nuclearly targeted GFP, together with 0.5 μg of empty control vector (pEF1) or a plasmid expressing the baculovirus p35 (pCAGGS-p35), cowpox virus crmA (pEF1-crmA), or human Bcl-2 gene (pEF1-hBcl2). Cells were then cultured in medium containing 0.6 mM glucose for 48 h. Percentage apoptosis was scored in GFP-expressing cells by examining their nuclear morphology under the fluorescence microscope (see Fig. S1). Data represent the mean ± SE of 6 independent experiments. *$p < 0.001$ vs pEF1.

whether or not this applies to beta cell death induced by low glucose or AICAR. Culture under either condition increased caspase-3 activity in Neo^R control MIN6 cells, whereas this response was suppressed in Neo^R MIN6 cells exhibiting hBcl-2 expression (Fig. 9A). Immunoblotting showed a clear processing of pro-casp-3 (32 kDa) in Neo^R control cells in response to the apoptotic conditions, whereas casp-3 was not processed in Neo^R cells that expressed hBcl-2 (Fig. 9B). In the latter, endogenous (mouse) Bcl-2 protein was also no longer truncated to 24 kDa (Fig. 9B). AMPK and JNK activation are early signals that contribute to the apoptosis pathway [3–5,8]. In keeping with this, hBcl-2 expression did not prevent activation of these kinases in MIN6 cells exposed to AICAR (Fig. 9C). The results indicate that casp-3-activation and truncation of endogenous Bcl-2 occur downstream of the point of action of hBcl-2 in the apoptosis pathway. Together our data suggest that early mitochondrial dysfunction and ROS formation contribute to apoptosis initiation while casp-3 and Bcl-2 processing may amplify the mitochondrial death signal.

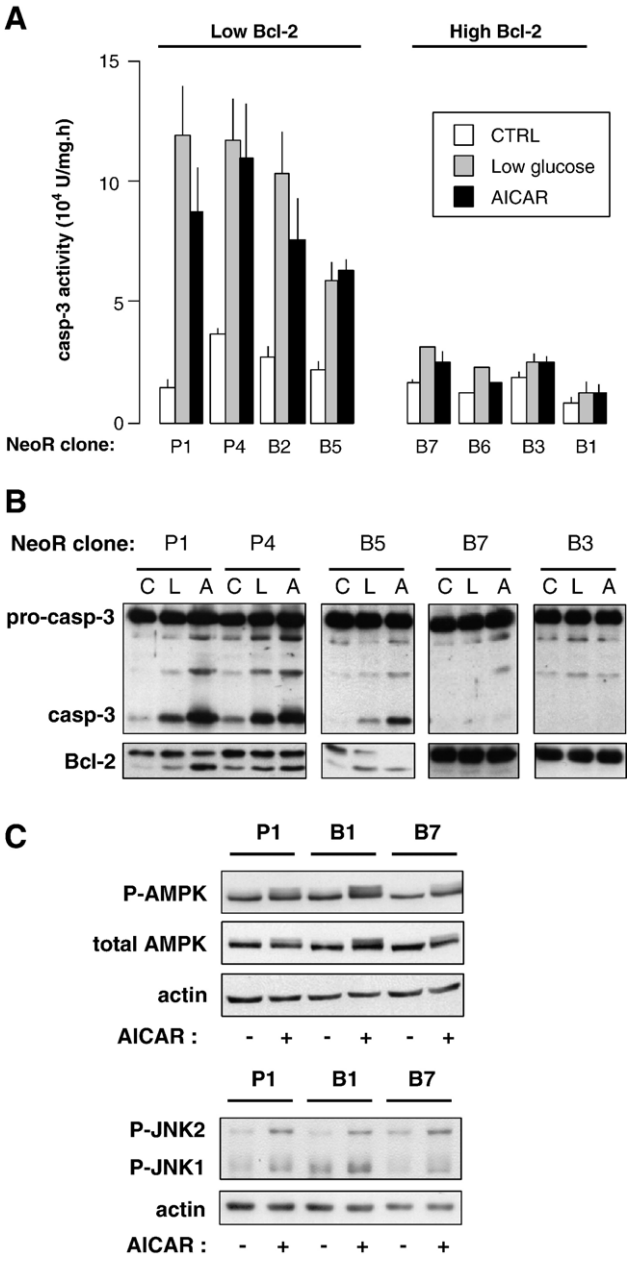

Fig. 9. hBcl-2 expression prevents proteolytic activation of caspase-3 and cleavage of endogenous Bcl-2 in MIN6 cells, but does not influence AMPK and JNK phosphorylation. (A) The Neo^R cells were treated as in Fig. 6, and specific activity (U/mg h) of casp-3 was measured fluorometrically (see Materials and methods). Data represent mean ± SE of 4 independent experiments. (B) Cells (as in A) were analyzed by Western blotting for conversion of pro-casp-3 (32 kDa) to active casp-3 (17 kDa), and for truncation of endogenous (mouse) Bcl-2. (C=CTRL, L=low glucose, A=AICAR). B3 and B7 cells, with high level h-Bcl-2 expression, showed no casp-3 processing, nor truncation of endogenous Bcl-2. Anti-mouse Bcl-2 antibody cross-reacted with high levels of the human Bcl-2 protein in B3 and B7. (C) Phosphorylation of AMPK (p-AMPK) and JNK (p-JNK1 and 2) was studied by Western blotting in B1- and B7 cells with high level h-Bcl-2 expression and in P1 cells negative for hBcl-2. Phosphorylation was induced by 4-h culture in 2 mM AICAR. Blots shown are respresentative of 3 experiments.

Discussion

Recently, we demonstrated that acute reduction of glucose metabolism stimulates the mitochondrial ROS production in purified rat beta cells. This effect was explained by decreased mitochondrial metabolic rate, and an associated oxidized state of flavin (FAD/FMN) cofactors in the electron transport chain resulting in superoxide formation [24]. In the present study we examined the mechanistic contribution of ROS to cell death induced by sustained AMPK activation in MIN6 cells (1) cultured in a low glucose concentration or (2) in the presence of AICAR.

ROS generation was measured with two probes, namely the sensitive but unspecific H_2-DCF that is oxidized by various peroxide-like ROS but also by nitric oxide-derived reactive species [35], and the superoxide-selective probe, DHE [36]. The oxidation of both probes was increased following a sustained exposure to low glucose or AICAR. The observation that ROS scavengers that reduced the DHE oxidation (superoxide) proportionately reduced H_2-DCF oxidation shows that both probes detect radicals derived from a single source. The most plausible scheme is that this source is superoxide, primarily generated at the electron transport chain. Subsequent formation of complex peroxide species, dismutation of superoxide to H_2O_2-compatible with the concomitant increase in catalase expression-and/or formation of peroxynitrite then result in H_2-DCF oxidation. Additional proof for this sequence of events comes from the fact that the strictly mitochondrial fuel pyruvate, which is taken up and metabolized by MIN6 cells [28], also prevented the accumulation of both superoxide and the DCF signals in low glucose-exposed cells. Glucose deprivation-induced ROS formation has previously been observed in breast cancer cell lines [41,42] and in HepG2 hepatoma cells [43]. The latter study also showed that ROS formation under conditions of glucose deprivation required a functional electron transport chain and that the mechanism can be considered as a novel mechanism of metabolic signaling, leading to the induction of various genes such as heme oxygenase-1. A novel finding in our study is that the AMPK activator AICAR also induced formation of superoxide (-derived ROS). That this was associated with

marked redox imbalances in mitochondrial electron transport (oxidized redox state of FAD/FMN cofactors) suggests a causal relationship. It is conceivable that semioxidized flavins are more prone to superoxide formation [44], which is also compatible with the earlier observed association of oxidized flavins with mitochondrial ROS in primary beta cells [24]. The increased ROS production under these conditions is indicative of a mitochondrial dysfunction. Our MTT assay data show that both low glucose and AICAR rapidly decrease the mitochondrial metabolic activity. Since several radical scavengers suppress the ROS accumulation in MIN6 cells and also significantly decrease cell death, we conclude that increased mitochondrial ROS generation is not an epiphenomenon of the cell death observed under the given culture conditions but is a mechanism which contributes to the apoptosis.

Our observations in MIN6 cells that-with a similar time course-both low glucose concentration and AICAR (1) enhanced superoxide production, (2) decreased mitochondrial activity (MTT assay), and (3) increased oxidation state of FAD/FMN suggest that AMPK activation can result in mitochondrial dysfunction. This is consistent with the results showing that both AICAR and low glucose markedly decreased glucose-oxidation and suppressed the glucose-induced insulin secretion in MIN6 cells. In view of the finding that the insulin stores were not increased in low glucose and were reduced in AICAR, the data are consistent with our earlier results showing that the AMPK activators metformin and AICAR decrease beta cell biosynthetic activity [5]. In addition, our data corroborate the observations made by others that expression of CA-AMPK results in decreased glucose oxidation, cellular [ATP], and insulin secretion, in mouse and rat pancreatic islets or MIN6 cells [6,7]. We conclude from these results that the suppression of glucose oxidation and beta cell function reflect an inhibitory action of AMPK on mitochondrial function. This inhibitory action, however, selectively affects the glucose branch of mitochondrial metabolism: even after a sustained period of exposure to low glucose and/or AICAR which resulted in suppressed glucose oxidation, protein biosynthesis inhibition, and ROS formation, palmitate oxidation was unaffected.

The notion that increased superoxide production can result from a decreased glucose metabolism is not new in beta cells [24], and was previously demonstrated in various other cell types [41–43]. Moreover, it was recently shown that increased ROS production by chronic hyperglycemia in beta cells was associated with-paradoxically-lowered glucose metabolism and decreased association of glucokinase with mitochondria [45]. It would be interesting to investigate whether AMPK activation by AICAR downregulates (mitochondrially associated) glucokinase: such action (1) would affect glucose metabolism similarly as when cells are exposed to a low glucose concentration, (2) could explain its specific inhibitory effect on glucose oxidation, (3) could help to clarify the mitochondrial ROS generation. Indeed, GK downregulation would not only decrease the formation of antioxidative NAD(P)H equivalents from glucose [46], but also preclude recycling of ADP at the mitochondria, resulting in state IV respiration, mitochondrial membrane hyperpolarization, and superoxide production [47,48]. An additional question which we have not adressed and which warrants further study in the present context is whether AMPK activation influences glucose utilization in beta cells.

It is at present unclear how AMPK activation causes redox imbalance with increased oxidized state of mitochondrial $FADH_2$/$FMNH_2$ but not total cellular NAD(P)H. Possibly, an AMPK-activated Randle effect is involved here: AMPK has been shown to be a strong activator of fatty acid beta-oxidation, in part chronically via PPAR alpha/PGC-1-mediated phenotypic adaptations [49]. Increased oxidation of fatty acids-which are present in serum-containing medium-will increase the mitochondrial acetyl-coA/coA ratio, and hence slow down the flux of glucose-derived pyruvate through the pyruvate dehydrogenase complex (PDH) [50,51]. Such a metabolic scenario has been shown to evolve gradually with time in beta cells after prolonged fasting, and has been implied in the decreased glucose oxidation in beta cells under this condition [51]. Glucose carbon will then be shunted away from oxidation, via pyruvate carboxylase, to malate which then participates in NAD(P)H-generating reactions in the cytoplasm [50]. Palmitate oxidation in MIN6/beta cells, in terms of carbon equivalents oxidized, is low as compared to glucose oxidation (our data, Fig. 2), and is thus expected to generate limited amounts of mitochondrial NADH/$FADH_2$ and ATP, which entails a shut-down of GSIS via inactivation of the triggering, K^+_{ATP}-dependent pathway of GSIS [52]. If this occurs in MIN6 cells chronically exposed to AICAR, and/or glucose deprivation, the oxidized mitochondrial flavins would represent a combination of oxidized soluble Krebs cycle FAD, FMN in electron transport chain I, and FAD in the PDH complex. While flavins are mainly mitochondrial, our NAD(P)H measurements reflect both cytoplasmic and mitochondrial levels. In normal, glucose-stimulated beta cells there is a close equilibration between mitochondrial NADH and $FADH_2$ [53]. Together, this leaves the possibility that in AICAR-exposed MIN6 cells the decreased glucose oxidation is in fact accompanied, not only by decreased mitochondrial $FADH_2$/$FMNH_2$ but also by decreased NADH, the latter masked by increased cytoplasmic NAD(P)H. Such a scenario can also explain the markedly decreased mitochondrial redox potential, measured by MTT assay. An oxidized state of mitochondrial NADH and FAD/FMN in beta cells was previously associated with increased oxygen radical formation from an oxidized FMN or associated Fe-S cluster in complex I [24]. Ultimately, the combination of ATP depletion, inhibited protein synthesis and mitochondrial ROS formation creates a vicious cycle, secondarily slowing down beta oxidation despite its intrinsic stimulation by AMPK. This model (see Fig. 10) predicts that pharmacological inhibition of beta-oxidation in AICAR-exposed MIN6 might partially correct the observed AICAR suppression of glucose oxidation, as was previously shown for fasting-induced suppression of glucose oxidation in beta cells [51].

It was previously shown that JNK is a mediator of apoptosis induction by AICAR or CA-AMPK in MIN6 cells [4]. Both JNK and its downstream target, c-Jun, are also activated in MIN6 cells cultured in low glucose concentrations [4]. In

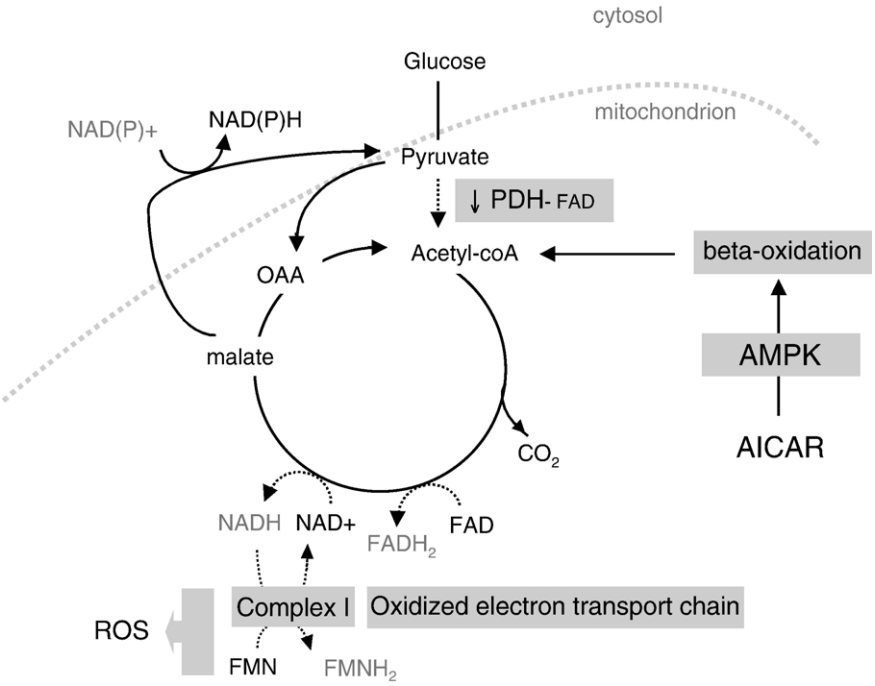

Fig. 10. Hypothetical mechanism of AICAR-induced inhibition of mitochondrial metabolism and $FADH_2$/NAD(P)H imbalance. AMPK activation stimulates fatty acid oxidation which leads to inhibition of pyruvate dehydrogenase (PDH) and glucose oxidation (Randle effect). This decreases mitochondrial NADH and $FADH_2$, favoring an oxidized state of the respiratory chain. This in turn leads to ROS formation through keeping FMN unsaturated in complex I, as previously proposed [24]. The pyruvate/malate shuttle generates cytosolic NADPH, leaving a relative deficiency of mitochondrial $FADH_2$ vs total NAD(P)H. Under sustained AMPK activation, however, ATP depletion, inhibition of protein synthesis, and mitochondrial oxygen radical formation then create a vicious cycle, causing general mitochondrial metabolic dysfunction, ultimately also affecting fatty acid oxidation.

hemapoietic progenitor cells and neurons, JNK and c-Jun have been implicated in initiation of apoptosis through transcriptional regulation of BH3-only genes, including DP-5 and Bim [54–56]. Proapoptotic BH3-only members of the Bcl-2 family can cooperate with BH3 containing proteins Bax and Bak to induce release of mitochondrial proteins such as cytochrome *c* [39]. While BH3-only members are subject to stringent control in normal cells, BH3-only subsets that are regulated at the RNA level can be promptly upregulated in response to apoptotic signals. A few genes, such as *hrk/dp5* [57,58], *noxa* [59], *puma/bbc3* [60,61], *bim* [62,63], and *bid* [64] are activated by transcription. However, activation of each of these genes was reported in non-beta-cell types ranging from primary cells (neurons, lymphocytes, thymocytes, colon) to tumor cells [57–64], and beta cells or MIN6 cells might respond differently. The present study examined the modulation of BH3-only proteins at the RNA level in beta cells and MIN6 cells. Our RT-PCR study showed that at 24 h, BH3-only mRNA encoding DP5 or Bim were upregulated, while antiapoptotic paralogs were either unaffected or downregulated under conditions of AMPK activation. The data suggest that increased expression of certain BH3-only members of the Bcl-2 family can contribute to apoptosis onset under conditions of AMPK activation. The observed upregulation of DP5 and Bim may constitute a functional link between JNK activation and cell execution in our models, although this requires further investigation.

The dysregulation of BH3 members of the Bcl-2 family observed in the present study suggests that activation of the intrinsic apoptosis pathway mediates beta cell death. This notion is supported by preventing apoptosis in MIN6 cells through stable expression of recombinant human Bcl-2 protein. The present analysis confirms the results of previous studies implicating the mitochondrial pathway in AICAR-induced apoptosis [11,65], and extends the finding to other conditions associated with sustained AMPK activation. AICAR triggers apoptosis independently of AMPK activation and ZMP synthesis in Jurkat cells [65], whereas AMPK activation contributes to AICAR-induced apoptosis in liver cells, beta cells, B-lymphocytes and gastric cancer cells [3,4,8,10,11]. Our study showing that two AMPK-activating conditions lead to mitochondrial dysfunction, together with the observations that pharmacological AMPK activators and CA-AMPK can decrease glucose oxidation in beta cells [5–7], strongly suggests that mitochondrial inhibition and ensuing ROS production are part of the AMPK-mediated apoptosis pathway. Since AMPK activation by low glucose or AICAR occurs rapidly [3,4], before ROS production is significantly increased in MIN6 cells (not shown), the ROS formation is not a likely stimulator of AMPK in our models. A contributory role of ROS species on the long-term activation of AMPK in beta cells can, however, not be excluded [66]. Our data show that the increased ROS production is an early event with respect to the apoptotic execution, since it was unaffected by enhanced Bcl-2 expression.

In both low glucose and AICAR, caspase-3 was proteolytically activated, an event that was paralleled by caspase-dependent truncation of the antiapoptotic regulator Bcl-2.

Caspase-mediated truncation of Bcl-2 has been demonstrated in other systems to yield a Bax-like death effector responsible for triggering apoptosis [40]. Our study therefore suggests that Bcl-2 truncation can contribute to apoptosis of beta cells under these culture conditions. This is supported by the observation that transient transfection of plasmids encoding either human Bcl-2 or baculovirus p35, a selective inhibitor of casp-3, both inhibited MIN6 cell death. To examine whether the observed processing of caspase-3 and Bcl-2 acts proximally or distally in the apoptosis program, MIN6 cells were studied that stably express the human Bcl-2 protein. When the cells were exposed to either low glucose or AICAR for up to 48 h they remained viable and did not exhibit casp-3 processing or activation, nor truncation of recombinant or endogenous Bcl-2. This indicates that the processing of casp-3 and Bcl-2 occurs distally with respect to the antiapoptotic action of Bcl-2. In contrast, phosphorylation of AMPK and JNK was not inhibited by ectopic Bcl-2 expression, which is in agreement with the proximal role of these kinases in the apoptosis pathway [4,8].

In conclusion, the present data suggest that AMPK activation in beta cells leads to mitochondrial dysfunction and increased ROS production, which contributes to activation of the intrinsic mitochondrial apoptosis pathway. Processing of Bcl-2 participates in amplification rather than initiation of beta cell death.

Acknowledgments

We thank Geert Stangé, Karen Kerckhofs, and Gabriël Schoonjans, for excellent technical assistance. This work was supported by Grants from the Scientific Research Fund Flanders (FWO-G.0357.03 and 101/8 to G.M., who is aspirant FWO), by the Inter-University Poles of Attraction Program (IUAP P5/17) from the Belgian Science Policy, and by the Brussels Free University, VUB (OZR-898 and 1161). S.H. is a Canadian Institutes of Health Research postdoctoral fellow.

Appendix A. Supplementary data

Supplementary data associated with this article can be found, in the online version, at doi:10.1016/j.freeradbiomed.2006.09.018.

References

[1] Hoorens, A.; Van de Casteele, M.; Kloppel, G.; Pipeleers, D. Glucose promotes survival of rat pancreatic beta cells by activating synthesis of proteins which suppress a constitutive apoptotic program. *J. Clin. Invest.* **98:**1568–1574; 1996.

[2] Salt, I. P.; Johnson, G.; Ashcroft, S. J.; Hardie, D. G. AMP-activated protein kinase is activated by low glucose in cell lines derived from pancreatic beta cells, and may regulate insulin release. *Biochem. J.* **335:**533–539; 1998.

[3] Kefas, B. A.; Heimberg, H.; Vaulont, S.; Meisse, D.; Hue, L.; Pipeleers, D.; Van de Casteele, M. AICA-riboside induces apoptosis of pancreatic beta cells through stimulation of AMP-activated protein kinase. *Diabetologia* **46:**250–254; 2003.

[4] Kefas, B. A.; Cai, Y.; Ling, Z.; Heimberg, H.; Hue, L.; Pipeleers, D.; Van de Casteele, M. AMP-activated protein kinase can induce apoptosis of insulin producing MIN6 cells through stimulation of c-jun-N-terminal kinase. *J. Mol. Endocrinol.* **30:**151–161; 2003.

[5] Kefas, B. A.; Cai, Y.; Kerckhofs, K.; Ling, Z.; Martens, G.; Heimberg, H.; Pipeleers, D.; Van de Casteele, M. Metformin-induced stimulation of AMP-activated protein kinase in beta-cells impairs their glucose responsiveness and can lead to apoptosis. *Biochem. Pharmacol.* **68:**409–416; 2004.

[6] da Silva Xavier, G.; Leclerc, I.; Varadi, A.; Tsuboi, T.; Moule, S. K.; Rutter, G. A. Role for AMP-activated protein kinase in glucose-stimulated insulin secretion and preproinsulin gene expression. *Biochem. J.* **371:**761–774; 2003.

[7] Richards, S. K.; Parton, L. E.; Leclerc, I.; Rutter, G. A.; Smith, R. M. Over-expression of AMP-activated protein kinase impairs pancreatic {beta}-cell function in vivo. *J. Endocrinol.* **187:**225–235; 2005.

[8] Meisse, D.; Van de Casteele, M.; Beauloye, C.; Hainault, I.; Kefas, B. A.; Rider, M. H.; Foufelle, F.; Hue, L. Sustained activation of AMP-activated protein kinase induces c-Jun N-terminal kinase activation and apoptosis in liver cells. *FEBS Lett.* **526:**38–42; 2002.

[9] Garcia-Gil, M.; Pesi, R.; Perna, S.; Allegrini, S.; Giannecchini, M.; Camici, M.; Tozzi, M. G. 5′-Aminoimidazole-4-carboxamide riboside induces apoptosis in human neuroblastoma cells. *Neuroscience* **117:** 811–820; 2003.

[10] Campas, C.; Lopez, J. M.; Santidrian, A. F.; Barragan, M.; Bellosillo, B.; Colomer, D.; Gil, J. Acadesine activates AMPK and induces apoptosis in B-cell chronic lymphocytic leukemia cells but not in T lymphocytes. *Blood* **101:**3674–3680; 2003.

[11] Saitoh, M.; Nagai, K.; Nakagawa, K.; Yamamura, T.; Yamamoto, S.; Nishizaki, T. Adenosine induces apoptosis in the human gastric cancer cells via an intrinsic pathway relevant to activation of AMP-activated protein kinase. *Biochem. Pharmacol.* **67:**2005–2011; 2004.

[12] McCullough, L. D.; Zeng, Z.; Li, H.; Landree, L. E.; McFadden, J.; Ronnett, G. V. Pharmacological inhibition of AMP-activated protein kinase provides neuroprotection in stroke. *J. Biol. Chem.* **280:**20493–20502; 2005.

[13] Hardie, D. G.; Carling, D. The AMP-activated protein kinase–fuel gauge of the mammalian cell? *Eur. J. Biochem.* **246:**259–273; 1997.

[14] Horman, S.; Browne, G.; Krause, U.; Patel, J.; Vertommen, D.; Bertrand, L.; Lavoinne, A.; Hue, L.; Proud, C.; Rider, M. Activation of AMP-activated protein kinase leads to the phosphorylation of elongation factor 2 and an inhibition of protein synthesis. *Curr. Biol.* **12:**1419–1423; 2002.

[15] Hardie, D. G.; Scott, J. W.; Pan, D. A.; Hudson, E. R. Management of cellular energy by the AMP-activated protein kinase system. *FEBS Lett.* **546:**113–120; 2003.

[16] Stefanelli, C.; Stanic, I.; Bonavita, F.; Flamigni, F.; Pignatti, C.; Guarnieri, C. Caldarera, CM. Inhibition of glucocorticoid-induced apoptosis with 5-aminoimidazole-4-carboxamide ribonucleoside, a cell-permeable activator of AMP-activated protein kinase. *Biochem. Biophys. Res. Commun.* **243:**821–826; 1998.

[17] Blazquez, C.; Geelen, M. J.; Velasco, G.; Guzman, M. The AMP-activated protein kinase prevents ceramide synthesis de novo and apoptosis in astrocytes. *FEBS Lett.* **489:**149–153; 2001.

[18] Culmsee, C.; Monnig, J.; Kemp, B. E.; Mattson, M. P. AMP-activated protein kinase is highly expressed in neurons in the developing rat brain and promotes neuronal survival following glucose deprivation. *J. Mol. Neurosci.* **17:**45–58; 2001.

[19] Ido, Y.; Carling, D.; Ruderman, N. Hyperglycemia-induced apoptosis in human umbilical vein endothelial cells: inhibition by the AMP-activated protein kinase activation. *Diabetes* **51:**159–167; 2002.

[20] Inoki, K.; Zhu, T.; Guan, K. L. TSC2 mediates cellular energy response to control cell growth and survival. *Cell* **115:**577–590; 2003.

[21] Marchetti, P.; Del Guerra, S.; Marselli, L.; Lupi, R.; Masini, M.; Pollera, M.; Bugliani, M.; Boggi, U.; Vistoli, F.; Mosca, F.; Del Prato, S. Pancreatic islets from type 2 diabetic patients have functional defects and increased apoptosis that are ameliorated by metformin. *J. Clin. Endocrinol. Metab.* **89:**5535–5541; 2004.

[22] Luo, Z.; Saha, A. K.; Xiang, X.; Ruderman, N. B. AMPK, the metabolic syndrome and cancer. *Trends Pharmacol. Sci.* **26:**69–76; 2005.

[23] Rutter, G. A.; Da Silva Xavier, G.; Leclerc, I. Roles of 5′-AMP-activated protein kinase (AMPK) in mammalian glucose homoeostasis. *Biochem. J.* **375:**1–16; 2003.

[24] Martens, G. A.; Cai, Y.; Hinke, S.; Stange, G.; Van de Casteele, M.; Pipeleers, D. Glucose suppresses superoxide generation in metabolically responsive pancreatic beta cells. *J. Biol. Chem.* **280:**20389–20396; 2005.

[25] Pipeleers, D. G.; in't Veld, P. A.; Van de Winkel, M.; Maes, E.; Schuit, F. C.; Gepts, W. A new in vitro model for the study of pancreatic A and B cells. *Endocrinology* **117:**806–816; 1985.

[26] Ling, Z.; Pipeleers, D. G. Preservation of glucose-responsive islet beta-cells during serum-free culture. *Endocrinology* **134:**2614–2621; 1994.

[27] Van de Casteele, M.; Kefas, B. A.; Ling, Z.; Heimberg, H.; Pipeleers, D. G. Specific expression of Bax-omega in pancreatic beta-cells is down-regulated by cytokines before the onset of apoptosis. *Endocrinology* **143:**320–326; 2002.

[28] Van de Casteele, M.; Kefas, B. A.; Cai, Y.; Heimberg, H.; Scott, D. K.; Henquin, J. C.; Pipeleers, D.; Jonas, J. C. Prolonged culture in low glucose induces apoptosis of rat pancreatic beta-cells through induction of c-myc. *Biochem. Biophys. Res. Commun.* **312:**937–944; 2003.

[29] Schuit, F. C.; In't Veld, P. A.; Pipeleers, D. G. Glucose stimulates proinsulin biosynthesis by a dose-dependent recruitment of pancreatic beta cells. *Proc. Natl. Acad. Sci. USA* **85:**3865–3869; 1988.

[30] Van De Winkel, M.; Pipeleers, D. Autofluorescence-activated cell sorting of pancreatic islet cells: purification of insulin-containing B-cells according to glucose-induced changes in cellular redox state. *Biochem. Biophys. Res. Commun.* **114:**835–842; 1983.

[31] Janjic, D.; Wollheim, C. B. Islet cell metabolism is reflected by the MTT (tetrazolium) colorimetric assay. *Diabetologia* **35:**482–485; 1992.

[32] Segu, V. B.; Li, G.; Metz, S. A. Use of a soluble tetrazolium compound to assay metabolic activation of intact beta cells. *Metabolism* **47:**824–830; 1998.

[33] Nicoletti, I.; Migliorati, G.; Pagliacci, M. C.; Grignani, F.; Riccardi, C. A rapid and simple method for measuring thymocyte apoptosis by propidium iodide staining and flow cytometry. *J. Immunol. Methods* **139:**271–279; 1991.

[34] Heimberg, H.; Bouwens, L.; Heremans, Y.; Van De Casteele, M.; Lefebvre, V.; Pipeleers, D. Adult human pancreatic duct and islet cells exhibit similarities in expression and differences in phosphorylation and complex formation of the homeodomain protein Ipf-1. *Diabetes* **49:**571–579; 2000.

[35] LeBel, C. P.; Ischiropoulos, H.; Bondy, S. C. Evaluation of the probe 2′,7′-dichlorofluorescin as an indicator of reactive oxygen species formation and oxidative stress. *Chem. Res. Toxicol.* **5:**227–231; 1992.

[36] Bindokas, V. P.; Jordan, J.; Lee, C. C.; Miller, R. J. Superoxide production in rat hippocampal neurons: selective imaging with hydroethidine. *J. Neurosci.* **16:**1324–1336; 1996.

[37] Zhao, H.; Kalivendi, S.; Zhang, H.; Joseph, J.; Nithipatikom, K.; Vasquez-Vivar, J.; Kalyanaraman, B. Superoxide reacts with hydroethidine but forms a fluorescent product that is distinctly different from ethidium: potential implications in intracellular fluorescence detection of superoxide. *Free Radic. Biol. Med.* **34:**1359–1368; 2003.

[38] Pileggi, A.; Molano, R. D.; Berney, T.; Cattan, P.; Vizzardelli, C.; Oliver, R.; Fraker, C.; Ricordi, C.; Pastori, R. L.; Bach, F. H.; Inverardi, L. Heme oxygenase-1 induction in islet cells results in protection from apoptosis and improved in vivo function after transplantation. *Diabetes* **50:**1983–1991; 2001.

[39] Scorrano, L.; Korsmeyer, S. J. Mechanisms of cytochrome c release by proapoptotic BCL-2 family members. *Biochem. Biophys. Res. Commun.* **304:**437–444; 2003.

[40] Cheng, E. H. Y.; Kirsch, D. G.; Clem, R. J.; Ravi, R.; Kastan, M. B.; Bedi, A.; Ueno, K.; Hardwick, J. M. Conversion of Bcl-2 to a Bax-like death effector by caspases. *Science* **278:**1966–1968; 1997.

[41] Lee, Y. J.; Galoforo, S. S.; Berns, C. M.; Chen, J. C.; Davis, B. H.; Sim, J. E.; Corry, P. M.; Spitz, D. R. Glucose deprivation-induced cytotoxicity and alterations in mitogen-activated protein kinase activation are mediated by oxidative stress in multidrug-resistant human breast carcinoma cells. *J. Biol. Chem.* **273:**5294–5299; 1998.

[42] Blackburn, R. V.; Spitz, D. R.; Liu, X.; Galoforo, S. S.; Sim, J. E.; Ridnour, L. A.; Chen, J. C.; Davis, B. H.; Corry, P. M.; Lee, Y. J. Metabolic oxidative stress activates signal transduction and gene expression during glucose deprivation in human tumor cells. *Free Radic. Biol. Med.* **26:**419–430; 1999.

[43] Chang, S. H.; Garcia, J.; Melendez, J. A.; Kilberg, M. S.; Agarwal, A. Haem oxygenase 1 gene induction by glucose deprivation is mediated by reactive oxygen species via the mitochondrial electron-transport chain. *Biochem. J.* **371:**877–885; 2003.

[44] Massey, V. Activation of molecular oxygen by flavins and flavoproteins. *J. Biol. Chem.* **269:**22459–22462; 1994.

[45] Kim, W. H.; Lee, J. W.; Suh, Y. H.; Hong, S. H.; Choi, J. S.; Lim, J. H.; Song, J. H.; Gao, B.; Jung, M. H. Exposure to chronic high glucose induces beta-cell apoptosis through decreased interaction of glucokinase with mitochondria: downregulation of glucokinase in pancreatic beta-cells. *Diabetes* **54:**2602–2611; 2005.

[46] Pipeleers, D.; Van de Winkel, M. Pancreatic B cells possess defense mechanisms against cell-specific toxicity. *Proc. Natl. Acad. Sci. USA* **83:**5267–5271; 1986.

[47] da-Silva, W. S.; Gomez-Puyou, A.; de Gomez-Puyou, M. T.; Moreno-Sanchez, R.; De Felice, F. G.; de Meis, L.; Oliveira, M. F.; Galina, A. Mitochondrial bound hexokinase activity as a preventive antioxidant defense: steady-state ADP formation as a regulatory mechanism of membrane potential and reactive oxygen species generation in mitochondria. *J. Biol. Chem.* **279:**39846–39855; 2004.

[48] Korshunov, S. S.; Skulachev, V. P.; Starkov, A. A. High protonic potential actuates a mechanism of production of reactive oxygen species in mitochondria. *FEBS Lett.* **416:**15–18; 1997.

[49] Lee, W. J.; Kim, M.; Park, H. S.; Kim, H. S.; Jeon, M. J.; Oh, K. S.; Koh, E. H.; Won, J. C.; Kim, M. S.; Oh, G. T.; Yoon, M.; Lee, K. U.; Park, J. Y. AMPK activation increases fatty acid oxidation in skeletal muscle by activating PPARalpha and PGC-1. *Biochem. Biophys. Res. Commun.* **340:**291–295; 2006.

[50] Zhou, Y. P.; Grill, V. E. Long-term exposure of rat pancreatic islets to fatty acids inhibits glucose-induced insulin secretion and biosynthesis through a glucose fatty acid cycle. *J. Clin. Invest.* **93:**870–876; 1994.

[51] Zhou, Y. P.; Priestman, D. A.; Randle, P. J.; Grill, V. E. Fasting and decreased B cell sensitivity: important role for fatty acid-induced inhibition of PDH activity. *Am. J. Physiol.* **270:**E988–E994; 1996.

[52] Henquin, J. C. Triggering and amplifying pathways of regulation of insulin secretion by glucose. *Diabetes* **49:**1751–1760; 2000.

[53] Rocheleau, J. V.; Head, W. S.; Piston, D. W. Quantitative NAD(P)H/flavoprotein autofluorescence imaging reveals metabolic mechanisms of pancreatic islet pyruvate response. *J. Biol. Chem.* **279:**31780–31787; 2004.

[54] Sanz, C.; Benito, A.; Inohara, N.; Ekhterae, D.; Nunez, G.; Fernandez-Luna, J. L. Specific and rapid induction of the proapoptotic protein Hrk after growth factor withdrawal in hematopoietic progenitor cells. *Blood* **95:**2742–2747; 2000.

[55] Harris, C. A.; Johnson, E. M., Jr. BH3-only Bcl-2 family members are coordinately regulated by the JNK pathway and require Bax to induce apoptosis in neurons. *J. Biol. Chem.* **276:**37754–37760; 2001.

[56] Whitfield, J.; Neame, S. J.; Paquet, L.; Bernard, O.; Ham, J. Dominant-negative c-Jun promotes neuronal survival by reducing BIM expression and inhibiting mitochondrial cytochrome c release. *Neuron* **29:**629–643; 2001.

[57] Inohara, N.; Ding, L.; Chen, S.; Nunez, G. Harakiri, a novel regulator of cell death, encodes a protein that activates apoptosis and interacts selectively with survival-promoting proteins Bcl-2 and Bcl-X(L). *EMBO J.* **16:**1686–1694; 1997.

[58] Imaizumi, K.; Morihara, T.; Mori, Y.; Katayama, T.; Tsuda, M.; Furuyama, T.; Wanaka, A.; Takeda, M.; Tohyama, M. The cell death-promoting gene DP5, which interacts with the BCL2 family, is induced during neuronal apoptosis following exposure to amyloid beta protein. *J. Biol. Chem.* **274:**7975–7981; 1999.

[59] Oda, E.; Ohki, R.; Murasawa, H.; Nemoto, J.; Shibue, T.; Yamashita, T.; Tokino, T.; Taniguchi, T.; Tanaka, N. Noxa, a BH3-only member of the Bcl-2 family and candidate mediator of p53-induced apoptosis. *Science* **288:**1053–1058; 2000.

[60] Han, J.; Flemington, C.; Houghton, A. B.; Gu, Z.; Zambetti, G. P.; Lutz, R. J.; Zhu, L.; Chittenden, T. Expression of bbc3, a proapoptotic BH3-only gene, is regulated by diverse cell death and survival signals. *Proc. Natl. Acad. Sci. USA* **98:**11318–11323; 2001.

[61] Nakano, N.; Vousden, K. PUMA a novel proapoptotic gene, is induced by p53. *Mol. Cell* **7:**683–694; 2001.

[62] Dijkers, P. F.; Medema, R. H.; Lammers, J. W.; Koenderman, L.; Coffer, P. J. Expression of the proapoptotic Bcl-2 family member Bim is regulated by the forkhead transcription factor FKHR-L1. *Curr. Biol.* **10:**1201–1204; 2000.

[63] Putcha, G. V.; Moulder, K. L.; Golden, J. P.; Bouillet, P.; Adams, J. A.; Strasser, A.; Johnson, E. M. Induction of BIM, a proapoptotic BH3-only BCL-2 family member, is critical for neuronal apoptosis. *Neuron* **29:** 615–628; 2001.

[64] Sax, J. K.; Fei, P.; Murphy, M. E.; Bernhard, E.; Korsmeyer, S. J.; El-Deiry, W. S. BID regulation by p53 contributes to chemosensitivity. *Nat. Cell Biol.* **4:**842–849; 2002.

[65] Lopez, J. M.; Santidrian, A. F.; Campas, C.; Gil, J. 5-Aminoimidazole-4-carboxamide riboside induces apoptosis in Jurkat cells, but the AMP-activated protein kinase is not involved. *Biochem. J.* **370:**1027–1032; 2003.

[66] Choi, S. L.; Kim, S. J.; Lee, K. T.; Kim, J.; Mu, J.; Birnbaum, M. J.; Soo Kim, S.; Ha, J. The regulation of AMP-activated protein kinase by H_2O_2. *Biochem. Biophys. Res. Commun.* **287:**92–97; 2001.